

Accepted Manuscript

Title: EFFECT OF PREPARATION PROTOCOL ON THE SURFACE ACIDITY OF MOLYBDENUM CATALYSTS SUPPORTED ON TITANIA AND ZIRCONIA

Author: Nacéra Lamine Amel Benadda Amar Djadoun Akila Barama Juliette Blanchard



PII: S1381-1169(16)30427-7
DOI: <http://dx.doi.org/doi:10.1016/j.molcata.2016.10.006>
Reference: MOLCAA 10068

To appear in: *Journal of Molecular Catalysis A: Chemical*

Received date: 30-6-2016
Revised date: 3-10-2016
Accepted date: 4-10-2016

Please cite this article as: Nacéra Lamine, Amel Benadda, Amar Djadoun, Akila Barama, Juliette Blanchard, EFFECT OF PREPARATION PROTOCOL ON THE SURFACE ACIDITY OF MOLYBDENUM CATALYSTS SUPPORTED ON TITANIA AND ZIRCONIA, *Journal of Molecular Catalysis A: Chemical* <http://dx.doi.org/10.1016/j.molcata.2016.10.006>

This is a PDF file of an unedited manuscript that has been accepted for publication. As a service to our customers we are providing this early version of the manuscript. The manuscript will undergo copyediting, typesetting, and review of the resulting proof before it is published in its final form. Please note that during the production process errors may be discovered which could affect the content, and all legal disclaimers that apply to the journal pertain.

EFFECT OF PREPARATION PROTOCOL ON THE SURFACE ACIDITY OF MOLYBDENUM CATALYSTS SUPPORTED ON TITANIA AND ZIRCONIA

Nacéra Lamine¹, Amel Benadda^{1,*}, Amar Djadoun², Akila Barama¹ and Juliette Blanchard³

1- Laboratoire des Matériaux Catalytiques et Catalyse en Chimie Organique, Faculté de Chimie, USTHB, BP32 El Alia, Bab Ezzouar, 16111, Algiers, Algeria.

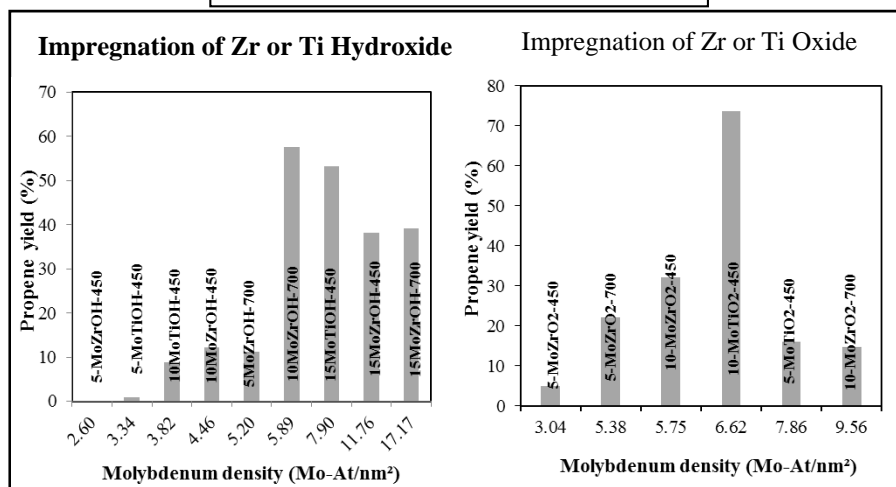
2- Laboratoire de Géophysique, FSTGAT, USTHB, BP 32, El Alia, Bab Ezzouar, 16111, Algiers, Algeria.

3- Sorbonne Universités, UPMC Univ Paris 6, UMR CNRS 7197, Laboratoire de Réactivité de Surface, F75005 Paris, France.

* Corresponding author. E-mail addresses: abenadda@usthb.dz ; benaddaamel@yahoo.fr.
(A.Benadda).

Graphical abstract

Isopropanol conversion at 120°C



Highlights

- Mo/TiO₂ and Mo/ZrO₂ were prepared via impregnation of metal hydroxides and oxides.
- The addition of Mo to the hydroxide or oxide leads to an increase of the surface area.
- At close Mo densities, the hydroxide impregnation leads to stronger acidity.
- The acid sites strength and density is optimal at Mo density about 6 Mo-At/nm².

Abstract

Molybdenum catalysts supported on titania and zirconia have been prepared via the impregnation on the corresponding hydroxides and oxides. The solids have been characterized by surface area measurements, XR-Fluorescence analysis, XRD and Raman Spectroscopy. The isopropanol decomposition reaction has been used to probe their acidic properties. These analyses revealed that introduction of molybdenum on the surfaces of the hydroxides and the oxides results in an increase of the specific surface area. Impregnation on the hydroxide leads to a comparatively better molybdenum dispersion and to a greater surface acidity. This indicates that the acid sites on hydroxide derived solids are stronger and more numerous than on their oxide derived counterpart.

Keywords: Molybdena; zirconium hydroxide; titanium hydroxide; impregnation; Isopropanol decomposition

1. Introduction

Molybdenum is an element that has been widely studied as catalyst component; it has been shown that, due to the electronic and structural properties of molybdenum oxides, they can be used as the main active phase or as an additive for many catalytic systems [1-3]. Indeed, molybdenum based catalysts are used in numerous industrial processes such as: olefins and alkynes metathesis, ammoxidation and oxidative dehydrogenation of light alkanes and hydrodesulphurization [4-11]. Molybdenum oxide is generally supported on metal oxides such as SiO_2 , Al_2O_3 , ZrO_2 , SnO_2 , MgO , CaO and TiO_2 in order to prevent its sintering. In these supported catalysts, the molybdenum constitutes the active phase and is dispersed on an oxide with a higher surface area. Molybdenum oxide-support interactions affect the structure and electronic properties of the active phase and influence therefore the catalytic performances of the solids. These interactions depend on the nature of the support, the active phase loading and the thermal treatment.

Titania and zirconia have been the object of great interest in the field of heterogeneous catalysis [12-17]. Both oxides are n-type semi-conductors and zirconia presents specific characteristics such as high thermal stability, extreme hardness, stability under reducing conditions and both acid and base functions whereas titania is well known to present SMSI properties as reported in early studies carried on Pt/TiO_2 and Ir/TiO_2 catalysts [16, 17].

Among supported molybdenum oxide, Mo/TiO_2 and Mo/ZrO_2 have been extensively studied [1, 2, 18-21]. Molybdenum sulfide supported on TiO_2 and ZrO_2 showed improved performances as hydrotreating catalysts thanks to higher dispersion and reducibility of molybdenum oxide phase when supported on titania and zirconia than on alumina and silica [2, 21-25]. In fact, the molybdenum species-support interactions depend on the acid-base properties of the support: the more basic the support, the stronger the interaction [26] and both TiO_2 and ZrO_2 are less acidic than Al_2O_3 . Moreover, Payen et al. have shown that the critical dispersion capacity for molybdenum oxo-species is higher on zirconia than on alumina [27].

Isopropanol decomposition has been widely used, among other test reactions, to probe acid-base properties of solid materials. It presents the advantage that dehydration; dehydrogenation and condensation reactions can occur simultaneously [28]. The analysis of the products distribution gives information about strength and density of catalysts' acid-base sites [29-31].

The purpose of the present work is to investigate the effect of the preparation method on the surface acidity of zirconia and titania supported molybdenum catalysts by means of the isopropanol decomposition test reaction.

2. Experimental

2.1. Catalyst preparation

The solids Mo/ZrO₂ and Mo/TiO₂ were prepared by the classic Ippatieff impregnation method [32] starting from zirconium/titanium hydroxides and oxides.

2.1.1 Support preparation

First, the oxyhydroxides ZrO_x(OH)_{4-2x} and TiO_x(OH)_{4-2x} were prepared starting from ZrOCl₂·8H₂O (Alfa Aesar 99.9%) and TiCl₄ (Merck 99%) respectively.

A 3M solution of TiCl₄ (pH=0.5) was prepared by adding pure TiCl₄ slowly to distilled water placed in an ice-water bath because the dissolution is very exothermic and may be explosive [33]. Ammonia solution (6N) was then added to the previous solution under stirring until the pH reached 9-10. For zirconium oxyhydroxide preparation, ammonia solution was added dropwise to a 0.5 M ZrO(NO₃)₂ solution (initial pH=2) until the pH reached 9.5. The resulting gels were aged for 24 hours then filtered and washed thoroughly with distilled water until the filtrate reached a neutral pH. The powders were lastly dried at 100°C overnight.

2.1.2 Catalyst preparation

For the first series of catalysts, Zr(OH)₄ and Ti(OH)₄ were dry impregnated with an aqueous solution of ammonium heptamolybdate (AHM) (NH₄)₆Mo₇O₂₄·4H₂O, provider : Strem Chemicals) whose concentration was adjusted in order to obtain different molybdenum loadings. The samples were dried at 100°C overnight and further calcined in air for 4 hours at 450 and 700°C for the Mo/ZrO₂ catalysts and at 450°C only for the Mo/TiO₂ systems. The solids of this series were labelled x-MoMOH-T where x represents the molybdenum loading, M the support cation symbol and T the calcination temperature.

For the second batch of catalysts, Zr(OH)₄ and Ti(OH)₄ were first calcined at 450°C for 4 hours before being used as supports. The obtained oxides were impregnated following the procedure used for the first series. The solids of this series are noted x-MoMO₂-T where x represents the molybdenum loading, M the support cation symbol and T the calcination temperature.

2.2. Catalyst characterization

All samples were characterized using the following physico-chemical methods:

Surface area measurements: Specific surface areas of samples (after outgassing during 1 h at 523 K under vacuum) were determined by nitrogen adsorption at 77 K on a Micromeritics ASAP 2060 system.

Powder X-ray diffraction (XRD): X-ray diffraction patterns were collected with a Philips diffractometer (type PW 1710) using $CuK\alpha$ radiation ($\lambda = 1,5418\text{\AA}$).

X-ray fluorescence analysis (XRF) : the molybdenum content was determined by X-ray fluorescence analyses conducted under He flow with an energy dispersive spectrometer (XEPOS with Turboquant powder software) equipped with a 50-Watt end-window X-ray tube to excite the samples.

Laser Raman spectroscopy: The Raman spectra were obtained using a BRUKER RAM II Raman spectrometer equipped with a Ge detector and using the 1064 nm excitation line of Nd-YAG laser. The data were collected by keeping the power at 30 mW and by recording 2000 scans per spectrum with a spectral resolution of 4 cm^{-1} .

2.3. Catalytic test

The isopropanol decomposition reaction was carried at 393 K in a fixed-bed continuous flow reactor under atmospheric pressure (see Supplementary information file) and in the absence of oxygen. Prior to catalytic tests, 0.05g of the solid was heated under flowing nitrogen at 250°C for 1 hour. The isopropanol was fed by flowing nitrogen ($40\text{ mL}\cdot\text{min}^{-1}$) through a saturator kept at 0°C to produce a pressure of 9 mmHg. The reaction was followed using on-line gas chromatography. Conversion and selectivities were calculated at steady state which was typically reached after less than 1 hour of reaction.

3. Results and discussion

3.1. X-Ray diffraction

3.1.1. Mo-Zr catalysts

Figure 1 depicts the XRD diffractograms of the solids supported on zirconia. Calcination of zirconium hydroxide at 450 and 700°C results in a mixture of monoclinic (m-ZrO₂) and tetragonal (t-ZrO₂), with a predominance of the monoclinic phase especially at 700°C (see table 1). This is consistent with previous studies which have shown that the metastable tetragonal phase was formed at low calcination temperatures, that its proportion was maximum 400°C and that it gradually declined after calcination at higher temperatures (up to 1200°C) due to its transformation into monoclinic zirconia [34, 35].

For the samples prepared by impregnation of Zr(OH)_4 with AHM, the tetragonal phase is the main form of zirconia whatever the calcination temperature. This clearly confirms that the molybdenum stabilizes the metastable tetragonal phase as reported in several studies [36, 37]. The tetragonal-monoclinic transformation at low temperatures has been proposed to occur via oxygen adsorption on specific sites, which seem to be also the anchoring sites for oxoanions such as sulfates and molybdates. Hence, the incorporation of oxoanions results in the inhibition of the phase transformation [38].

Considering the solids prepared by impregnation on ZrO_2 followed by calcination at 450°C , the diffractogram of the solid 5-MoZrO₂-450 is similar to the one of Zr(OH)_4 -450 with a predominance of the monoclinic zirconia phase, whereas, for the higher loading (10%), the proportion of tetragonal phase is higher than in the calcined support. At 700°C , the proportion of the tetragonal phase is more important in the solids containing molybdenum than in the support calcined at the same temperature.

For the solids supported on ZrO_2 , the calcination of the catalyst implies, for the zirconia phase, an additional thermal treatment at 450 or 700°C after the initial calcination step of Zr(OH)_4 at 450°C . This second thermal treatment results in a further crystallization of zirconia; the presence of molybdenum during this thermal treatment favors the formation of t- ZrO_2 at the expense of m- ZrO_2 , leading to an increase of the proportion of tetragonal phase in the Mo/ ZrO_2 solids compared to the support alone.

Weak XRD lines corresponding to MoO_3 were only observed on the pattern of the catalyst with the highest Mo loading (10% Mo), prepared by impregnation on ZrO_2 and calcined at 450°C .

$\text{Zr(MoO}_4)_2$ mixed oxide phase lines were observed on the diffractograms of the solids calcined at 700°C and with relatively high molybdenum loading, which is consistent with reported data in the literature [3,36].

3.1.2. Mo-Ti catalysts

The XRD patterns of the calcined catalysts prepared by using either Ti(OH)_4 or TiO_2 as support (Figure 2) indicate, for all Mo loading and independently of preparation protocol, a high dispersion of molybdenum on the support as no peaks except those of the anatase phase were observed.

3.2. Surface area measurements and elementary analysis

The molybdenum contents, BET surface areas and molybdenum surface densities of the Mo-Zr and Mo-Ti catalysts are shown in Table 1. The N₂ adsorption-desorption isotherms and pore size distributions of selected samples are given in the Supplementary information file.

Whatever the preparation protocol and the calcination temperature, the introduction of molybdenum on zirconium hydroxide or oxide resulted in a greater surface area of the catalyst compared to the support. Moreover, within one preparation protocol, the greater the molybdenum loading is, the higher the surface area of the supported solid. Additionally, the areas of the solids prepared by impregnation on Zr(OH)₄ are superior to those of the solids prepared by impregnation on ZrO₂.

The larger surface area of molybdenum supported on Zr(OH)₄ compared to Zr(OH)₄ alone after calcination at the same temperature has been widely commented in the literature [39, 40]. It has been proposed that promoters (cations or anions) decrease the sintering and grain-growth rates of zirconia, which results in a greater surface area and a hindrance of the tetragonal-monoclinic transformation [40]. Conversely, the increase of the surface area of an oxide after its impregnation by another component is not common. Indeed, it is generally admitted that impregnation results in a decrease of the surface, because (i) the active phase contributes to the overall weight of the catalyst and hence decreases the surface area by the mere fact that the proportion of high surface area support is lower in the catalyst than in the starting support; (ii) the active phase may partially block the support pores. We believe that as molybdenum exists as large oxo-species in the impregnation solution and as the zirconia has been prepared in the laboratory at mild conditions (calcination of Zr(OH)₄ at 450°C for 4 hours), the interaction between the oxygen atoms of the oxo-species and the zirconia surface defects may result in the de-agglomeration of zirconia particles leading to an increase of the surface area.

Similarly to the Mo-ZrOH solids, the surface areas of the Mo-TiOH systems are larger than that of the pure TiO₂ obtained by calcination of the titanium hydroxide at the same temperature. Hence, the presence of molybdenum also reduces the titania grain growth during the thermal treatment of the titanium hydroxide.

For the samples supported on TiO₂, a decrease in the specific surface area of the sample is first noted upon the impregnation of the support with 5 wt% of molybdenum, then as the molybdenum content increases to 10 wt%, the surface area increases and becomes greater than the initial surface of the support. This finding is different from the results observed for the ZrO₂ supported solids, where the surface of the supported solids are, whatever the molybdenum loading, superior to the support surface area. This difference may be attributed to the difference in

crystallinity between ZrO₂ and TiO₂. Indeed, ZrO₂ seems, based on the broadness of the lines of ZrO₂ diffractogram, to be slightly less crystallized than TiO₂. This implies the existence of a larger number of surface defects which are responsible for the interaction of molybdenum oxo-species with the support and, therefore for the enlargement of the surface area of the supported solids compared to the supports. It is noteworthy that a non-monotonic variation of the surface area of titania supported solids with increasing transition metal loading has already been reported by Tsilomelekis and Halkides [41, 42].

3.3. Laser Raman spectroscopy analysis

Supported molybdenum oxide has been thoroughly studied by Raman spectroscopy in the literature; assignment of the Raman bands is based on a careful examination of these previous reports.

3.1.1. Mo-Zr solids calcined at 450°C

Figure 3.a presents the Raman spectra of the Mo-Zr systems calcined at 450°C. The bands present on all spectra (Figures 3a and 3b) at low wave number (612-645 cm⁻¹) are characteristic of the oxide (the one appearing at ca. 613 cm⁻¹ corresponds to m-ZrO₂ and the second one at ca. 640 cm⁻¹ corresponds to t-ZrO₂).

The bands appearing in the 950 and 996 cm⁻¹ range have been attributed to the stretching of terminal Mo=O bonds [43–47]; when this band appears at high wavenumber (ca. 990-997 cm⁻¹) and that is accompanied by a band at 819-820 cm⁻¹ [43,44], it is a strong indication of the formation of MoO₃ crystallites. These bands can even be observed at Mo concentration for which the crystallization of MoO₃ is not detectable by XRD due to their small size. Based on this, 10-MoZrOH-450, 15-MoZrOH-450 and 10-MoZrO₂-450 contain MoO₃ crystallites.

The band corresponding to $\nu(\text{Mo}=\text{O})$ modes in MoO₆ octahedra within polymolybdates is located at lower wavenumbers (ca. 974-978 cm⁻¹) and its exact position is very sensitive to the size of the polymolybdate cluster and to the degree of hydration [36,43,44,46]. It is associated with a band at ca. 870-885 cm⁻¹ that is due to Mo-O-Mo vibrations in two-dimensional polymolybdates [47–49]. From these assignments, the solids 5-Mo-ZrO₂-450, 10-MoZrO₂-450, 10-MoZrOH-450 and 15-MoZrOH-450 contain polymolybdates clusters.

The band corresponding to $\nu(\text{Mo}=\text{O})$ modes in isolated molybdates is located at even lower wavenumbers, ca. 956 cm⁻¹ [43,48]. Based on this, the solid 5-MoZrOH-450 contains isolated molybdates. The second band, observed at 821 cm⁻¹ on the spectrum of this solid may correspond to the antisymmetric vibration mode of Mo-O-Zr [43,50].

3.1.2 The solids Mo-Zr calcined at 700°C

Figure 3.b presents the Raman spectra of the Mo-Zr systems calcined at 700°C. For all these solids, the two bands characteristic of the formation of crystalline MoO₃ are absent. Instead, new bands at 940 and 740 cm⁻¹ are clearly visible. They have been assigned, together with a ν(Mo=O) stretching band at 996 cm⁻¹, to the formation of the mixed oxide Zr(MoO₄)₂ [43,44]. These three bands are clearly visible on the spectra of 10-MoZrOH, 15-MoZrOH and 10-MoZrO₂, i.e. for the solids having the highest molybdenum densities. Moreover the Raman spectra of these solids exhibit bands at 976-980, 950-966, 850-884 and 807-810 cm⁻¹. The first two bands were attributed to the stretching vibration mode of terminal Mo=O bonds within the polymolybdates and isolated molybdates respectively, the bands at 850-884 cm⁻¹ and 807-810 cm⁻¹ correspond to the antisymmetric vibration modes (Mo-O-Mo) and (Mo-O-Zr) respectively.

The spectra of the solids with the lowest molybdenum loading (5%) exhibit a broad band in the Mo=O stretching region. The broadness of this band indicates that it may be constituted by two bands corresponding to the Mo=O stretching bond in isolated molybdates and polymolybdates. The presence of the bands corresponding to the Mo-O-Zr and Mo-O-Mo stretching confirms the coexistence of both types of molybdates.

From the analysis of the Raman spectra, it can be concluded that molybdenum on zirconia exists as isolated molybdate species only at low molybdenum density. At 450°C, for intermediate to high Mo densities, polymolybates are observed, and also, at densities higher than 4.46 Mo-at/nm², crystalline MoO₃ is formed. At 700°C, the MoO₃ bands are absent and bands characteristic of Zr(MoO₄)₂ are observed at high loadings (molybdenum density ≥ 5.9 Mo-at/nm²) whereas bands characteristic of polymolybdates are observed at all loadings and bands of isolated molybdates are observed at low and intermediate loadings. 700°C is well above the Tammann temperature of MoO₃; hence, a thermal spreading of MoO₃ is expected to occur during thermal treatment at 700°C [51], which could explain why the samples calcined at 700°C contain, at the same Mo loading, a larger proportion of (poly)molybdate in interaction with the support (antisymmetric Mo-O-Zr vibration at 807-810 cm⁻¹) than those calcined at 450°C.

3.1.3 The solids Mo-Ti

The Raman spectra of the Mo-Ti solids are represented on Figure 4. They all have been normalized with respect to the strong band at 634 cm⁻¹ assigned to TiO₂ (Anatase).

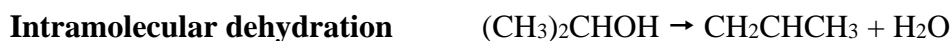
All the spectra displayed a band at 953-976 cm⁻¹; as the molybdenum density increases, this band is blue-shifted and its intensity increases. This band has been attributed to the stretching of terminal Mo=O bonds of surface molybdate species. For 5-MoTiOH-450 (i.e. the solid with the

lowest molybdenum density), this band is located at 953 cm^{-1} and could be assigned to the Mo=O stretching mode of isolated molybdates with a tetrahedral configuration [41,48].

As the molybdenum density increases, the $\nu(\text{Mo}=\text{O})$ band shifts to higher wavenumbers (ca. $968\text{-}976\text{ cm}^{-1}$). This can be explained by a growth of polymolybdates species with an octahedral coordination [48]. Additionally, new features appear at $\sim 815\text{-}820\text{ cm}^{-1}$ and 878 cm^{-1} . The band at 878 cm^{-1} is attributed to Mo-O-Mo linkages within polymolybdates species [48], whereas the band at $815\text{-}820\text{ cm}^{-1}$ is assigned to the antisymmetric stretching of Mo-O-Mo bonds within microcrystalline MoO_3 . Another band characteristic of MoO_3 is expected around 995 cm^{-1} . It is observed on the spectrum of 10-MoTiO₂ spectra (at ca. 991 cm^{-1}). It is however not clearly visible on the spectra of 5-MoTiO₂ and 15-MoTiOH but may be masked by the intense band at 976 cm^{-1} band for these two solids.

3.4. Isopropanol decomposition tests

The isopropanol (IPA) decomposition reaction has been widely used to probe acid-base and/or redox properties of catalysts depending on the reaction atmosphere[52]. Indeed, under inert atmosphere, the IPA undergoes dehydration leading to propene and diisopropylether over acid and/or basic sites and is dehydrogenated to acetone over basic sites according to the following reactions:



According to the literature, solid oxides with acidic character lead mainly to the formation of propene and diisopropylether; dehydrogenation reaction requires strong basic sites and occurs at temperatures above 573K [53]; propene formation necessitates strong acid sites [54,55] whereas the formation of diisopropylether involves weak acid sites [56]. The conversions and the selectivities for isopropanol decomposition reaction are reported in Table 2.

Bare supports, prepared by calcination of $\text{Zr}(\text{OH})_4$ and $\text{Ti}(\text{OH})_4$ at 450 or 700°C , are inactive at the reaction temperature chosen for this study. ZrO_2 and TiO_2 possess mainly Lewis acid sites associated with Zr^{4+} and Ti^{4+} ions [57,58]. Yet, these Lewis acid sites seem to be inactive towards the isopropanol decomposition at 120°C . This is likely due to the fact that, at moderate temperatures, the Lewis acid sites of oxides such as alumina, titania and zirconia are hydroxylated and hence their Lewis acidity is masked (replaced by the weak Brønsted acidity of the surface hydroxyls) and a thermal treatment above 300°C is required to reveal it [59–61]. Moreover, considering that the

isopropanol decomposition reaction produces water, even if a few Lewis sites were present after the pretreatment at 250°C, they would deactivate immediately by reaction with water molecules produced by the reaction. This finding is consistent with the results reported by Baertsch [62] who found that aluminium oxide is inactive in butanol dehydration reaction at 130°C despite the presence of Lewis acid sites.

The inactivity of the bare supports and the development of a catalytic activity upon the introduction of molybdenum on the support surfaces may indicate that the acid activity of the solids is mainly due to Brønsted acid sites in agreement with the conclusions of Samaranch et al. [63].

Besides the supports, all the supported catalysts, except 5-MoTiOH-450 and 5-MoZrOH-450, present an appreciable catalytic activity. Propene is the major product and the proportions of ether and acetone are very small on the most active catalysts. Only the samples with the lowest Mo loading (and hence the lowest activity) have significant selectivities towards ether and acetone.

Assuming that the formation of propene is directly related to the abundance of Brønsted acid sites, a correlation between the propene yield and the molybdenum density has been attempted (Figure 5). The correlation is quite good but not perfect as the propene yield happened to vary quite irregularly with the molybdenum density. A more careful look to Figure 5 reveals that the correlation between propene yield and molybdenum density is very good when considering the two preparation protocols separately (Figures 6.a & 6.b).

For the two preparation methods the maximum propene yield is obtained for the solids presenting a molybdenum density of about 6 Mo-At/nm². This indicates that these solids present the highest proportion of strong acid sites as the rate of dehydration to propene increases with the strength of the acid sites [60]. The solids with densities below 5 Mo-At/nm² present the lowest propene yields but exhibit at the same time the highest ether selectivities (Table 2). This clearly indicates that they contain weak acid sites as the dehydration to ether does not depend on the acid sites strength.

Hence, in addition to the molybdenum density, the preparation protocol affects the number and the strength of the created acid sites. Indeed, if we compare the propene yield obtained on solids presenting close molybdenum densities and supported on the same support, but synthesized via different protocols (Table 3), we observe that impregnation on the hydroxide leads always to a higher propene yield and hence to a surface with stronger acid sites.

Based on this, we can conclude that the variation of the concentration and strength of acid sites as a function of the molybdenum density and protocol preparation can be related to the structure of molybdenum species, as follows:

- **At very low molybdenum density (0-3.3 Mo-At/nm², Solids 5-MoZrOH-450, 5-MoTiOH-450 and 5-MoZrO₂-450):** the molybdenum exists mainly as isolated molybdates species and the activity of these solids is very low or null which means that isolated molybdates do not have Brønsted acid sites.
- **As molybdenum density increases (3.5-5.5 Mo/nm², Solids 10-MoTiOH-450, 10-MoZrOH-450, 5-MoZrOH-700, 5-MoZrO₂-700):** the molybdenum exists as polymolybdates and isolated molybdates. For these solids the isopropanol conversion is within 12-27% and the propene selectivity is between 63 and 83%, which indicates the formation of acid sites with different strength.
- **At molybdenum density close to 6 Mo-At/nm² (Solids 10-MoZrOH-700 and 10-MoTiO₂-450):** Raman spectroscopy and XRD have shown that these solids contain polymolybdates species with small amounts of microcrystalline MoO₃ for 10MoTiO₂-450 and Zr(MoO₄)₂ for 10-MoZrOH-700. These solids present the largest proportion of polymolybdates and led to the highest propene yield and hence have the most acid surfaces (in terms of number and strength of acid sites).
- **At High molybdenum surface densities (8-17 Mo/nm²):** the solids contain either crystalline MoO₃ and polymolybdates (5-MoTiO₂-450, 15-MoTiOH-450, 15-MoZrOH-450) or isolated molybdates, polymolybdates and large particles of mixed oxide Zr(MoO₄)₂ (10-MoZrO₂-700 and 15-MoZrOH-700). Involvement of part of the molybdenum in crystalline structures results in the diminution of the proportion of surface molybdate species and leads to a lower propene yield.

From the above discussion, we can conclude that the polymolybdates clusters are the molybdenum species responsible for the presence of strong Brønsted acid sites able to decompose isopropanol to propene. The optimum proportion of these polymolybdates is reached at a molybdenum density around 6 Mo-At/nm².

4. Conclusion

TiO₂ and ZrO₂ supported molybdenum oxide solids have been prepared by impregnation of ammonium heptamolybdate on the corresponding oxyhydroxide MO_x(OH)_{4-2x} and oxide MO₂.

An increase of the surface area has been observed upon the addition of molybdenum for most of the prepared solids. Moreover, the solids prepared by impregnation on the hydroxides have higher surface areas than the solids prepared by impregnation on the oxide. This has been assigned to an inhabitation of the grain-growth of the supports by the introduction of molybdenum; this grain-growth inhibition also hinders the tetragonal to monoclinic transformation for zirconia upon thermal

treatment. Raman spectroscopy allowed determining the speciation of molybdenum (isolated molybdate, polymolybdate, MoO_3 and $\text{Zr}(\text{MoO}_4)_2$) and was shown to better detect the formation crystalline MoO_3 than XRD. Raman spectroscopy especially showed that the polymerization of molybdenum species on the surface of the support is higher for the catalysts prepared with the oxides than with the oxyhydroxides.

The study of isopropanol decomposition led to the conclusion that, at comparable molybdenum densities, impregnation on the oxyhydroxide leads always to a surface with stronger acid sites. The strength and the density of acid sites are optimal at a molybdenum density of ca. 6 Mo-At/nm². The correlation between the structure of molybdenum species and the activity related to strong Brønsted acid sites (conversion of isopropanol to propene) allowed us concluding that the polymolybdates clusters are the molybdenum species responsible for the strong Brønsted acid sites and that the optimum proportion of these polymolybdates is reached at a molybdenum density of ca. 6 Mo-At/nm².

Funding

This work was supported by the Algerian Ministry of Higher Education and Scientific Research “MESRS” and USTHB Chemistry Faculty (PhD scholarship and Travel Grant for N. Lamine).

References

- [1] J. Ramírez, G. Macías, L. Cedeño, A. Gutiérrez-Alejandre, R. Cuevas, P. Castillo, The role of titania in supported Mo, CoMo, NiMo, and NiW hydrodesulfurization catalysts: analysis of past and new evidences, *Catal. Today*. 98 (2004) 19–30. doi:10.1016/j.cattod.2004.07.050.
- [2] M. Breysse, J.L. Portefaix, M. Vrinat, Support effects on hydrotreating catalysts, *Catal. Today*. 10 (1991) 489–505. doi:10.1016/0920-5861(91)80035-8.
- [3] P. Afanasiev, A. Thiollier, M. Breysse, J.L. Dubois, Control of the textural properties of zirconium oxide, *Top. Catal.* 8 (1999) 147–160. doi:10.1023/A:1019109127118.
- [4] R.R. Schrock, C. Czekelius, Recent Advances in the Syntheses and Applications of Molybdenum and Tungsten Alkylidene and Alkylidyne Catalysts for the Metathesis of Alkenes and Alkynes, *Adv. Synth. Catal.* 349 (2007) 55–77. doi:10.1002/adsc.200600459.
- [5] A.H. Hoveyda, A.R. Zhugralin, The remarkable metal-catalysed olefin metathesis reaction, *Nature*. 450 (2007) 243–251. doi:10.1038/nature06351.
- [6] R.K. Grasselli, J.D. Burrington, D.J. Buttrey, P. DeSanto, C.G. Lugmair, A.F. Volpe, T. Weingand, Multifunctionality of Active Centers in (Amm)oxidation Catalysts: From Bi–Mo–Ox to Mo–V–Nb–(Te, Sb)–Ox, *Top. Catal.* 23 (2003) 5–22. doi:10.1023/A:1024859917786.
- [7] M.O. Guerrero-Pérez, J.N. Al-Saeedi, V.V. Gulians, M.A. Bañares, Catalytic properties of mixed Mo–V–Sb–Nb–O oxides catalysts for the ammoxidation of propane to acrylonitrile, *Appl. Catal. Gen.* 260 (2004) 93–99. doi:10.1016/j.apcata.2003.10.004.

- [8] F. Cavani, F. Trifirò, The oxidative dehydrogenation of ethane and propane as an alternative way for the production of light olefins, *Catal. Today*. 24 (1995) 307–313. doi:10.1016/0920-5861(95)00051-G.
- [9] A. Christodoulakis, E. Heracleous, A.A. Lemonidou, S. Boghosian, An operando Raman study of structure and reactivity of alumina-supported molybdenum oxide catalysts for the oxidative dehydrogenation of ethane, *J. Catal.* 242 (2006) 16–25. doi:10.1016/j.jcat.2006.05.024.
- [10] S. Damyanova, L. Petrov, M.A. Centeno, P. Grange, Characterization of molybdenum hydrodesulfurization catalysts supported on ZrO₂-Al₂O₃ and ZrO₂-SiO₂ carriers, *Appl. Catal. Gen.* 224 (2002) 271–284. doi:10.1016/S0926-860X(01)00849-3.
- [11] S. Brunet, D. Mey, G. Pérot, C. Bouchy, F. Diehl, On the hydrodesulfurization of FCC gasoline: a review, *Appl. Catal. Gen.* 278 (2005) 143–172. doi:10.1016/j.apcata.2004.10.012.
- [12] B.S. Klose, F.C. Jentoft, R. Schlögl, In situ diffuse-reflectance infrared spectroscopic investigation of promoted sulfated zirconia catalysts during n-butane isomerization, *J. Catal.* 233 (2005) 68–80. doi:10.1016/j.jcat.2005.04.011.
- [13] T.N. Vu, J. van Gestel, J.P. Gilson, C. Collet, J.P. Dath, J.C. Duchet, Platinum tungstated zirconia isomerization catalysts: Part I. Characterization of acid and metal properties, *J. Catal.* 231 (2005) 453–467. doi:10.1016/j.jcat.2005.01.037.
- [14] D. A. Peña, B. S. Uphade, E. P. Reddy, P.G. Smirniotis, Identification of Surface Species on Titania-Supported Manganese, Chromium, and Copper Oxide Low-Temperature SCR Catalysts, *J. Phys. Chem. B*, 108 (2004) 9927–9936. doi:10.1021/JP0313122.
- [15] K.I. Hadjiivanov, D.G. Klissurski, Surface chemistry of titania (anatase) and titania-supported catalysts, *Chem. Soc. Rev.* 25 (1996) 61–69. doi:10.1039/cs9962500061.
- [16] S.J. Tauster, S.C. Fung, R.L. Garten, Strong metal-support interactions. Group 8 noble metals supported on titanium dioxide, *J. Am. Chem. Soc.* 100 (1978) 170–175. doi:10.1021/ja00469a029.
- [17] S.J. Tauster, S.C. Fung, Strong metal-support interactions: Occurrence among the binary oxides of groups IIA–VB, *J. Catal.* 55 (1978) 29–35. doi:10.1016/0021-9517(78)90182-3.
- [18] S. Badoga, R.V. Sharma, A.K. Dalai, J. Adjaye, Hydrotreating of heavy gas oil on mesoporous zirconia supported NiMo catalyst with EDTA, *Fuel*. 128 (2014) 30–38. doi:10.1016/j.fuel.2014.02.056.
- [19] K.V.R. Chary, K.R. Reddy, G. Kishan, J.W. Niemantsverdriet, G. Mestl, Structure and catalytic properties of molybdenum oxide catalysts supported on zirconia, *J. Catal.* 226 (2004) 283–291. doi:10.1016/j.jcat.2004.04.028.
- [20] P. Ciambelli, D. Sannino, V. Palma, V. Vaiano, Photocatalysed selective oxidation of cyclohexane to benzene on MoO_x/TiO₂, *Catal. Today*. 99 (2005) 143–149. doi:10.1016/j.cattod.2004.09.034.
- [21] M. Breyse, P. Afanasiev, C. Geantet, M. Vrinat, Overview of support effects in hydrotreating catalysts, *Catal. Today*. 86 (2003) 5–16. doi:10.1016/S0920-5861(03)00400-0.
- [22] C. Louis, J.-M. Tatibouët, M. Che, Catalytic properties of silica-supported molybdenum catalysts in methanol oxidation: The influence of molybdenum dispersion, *J. Catal.* 109 (1988) 354–366. doi:10.1016/0021-9517(88)90218-7.
- [23] M.A. Banares, J.L.G. Fierro, J.B. Moffat, The Partial Oxidation of Methane on MoO₃/SiO₂ Catalysts: Influence of the Molybdenum Content and Type of Oxidant, *J. Catal.* 142 (1993) 406–417. doi:10.1006/jcat.1993.1218.
- [24] S.K. Maity, M.S. Rana, S.K. Bej, J. Ancheyta-Juárez, G.M. Dhar, T.S.R.P. Rao, TiO₂-ZrO₂ mixed oxide as a support for hydrotreating catalyst, *Catal. Lett.* 72 (2001) 115–119. doi:10.1023/A:1009045412926.
- [25] J. Ramirez, S. Fuentes, G. Díaz, M. Vrinat, M. Breyse, M. Lacroix, Hydrodesulphurization activity and characterization of sulphided molybdenum and cobalt—molybdenum catalysts comparison of alumina, silica—alumina and titania supported catalysts, *Appl. Catal.* 52 (1989) 211–223. doi:10.1016/0166-9834(89)80004-1.

- [26] A.N. Desikan, L. Huang, S.T. Oyama, Structure and dispersion of molybdenum oxide supported on alumina and titania, *J. Chem. Soc. Faraday Trans.* 88 (1992) 3357–3365. doi:10.1039/FT9928803357.
- [27] E. Payen, L. Gengembre, F. Mauge, J.C. Duchet, J.C. Lavalley, Surface properties of zirconia catalyst carriers : interaction with oxomolybdates species, *Catal. Today.* 10 (1991) 521–539. doi:10.1016/0920-5861(91)80037-A.
- [28] J.A. Wang, X. Bokhimi, O. Novaro, T. López, F. Tzompantzi, R. Gómez, J. Navarrete, M.E. Llanos, E. López-Salinas, Effects of structural defects and acid–basic properties on the activity and selectivity of isopropanol decomposition on nanocrystallite sol–gel alumina catalyst, *J. Mol. Catal. Chem.* 137 (1999) 239–252. doi:10.1016/S1381-1169(98)00077-6.
- [29] R. Valarivan, C.N. Pillai, C.S. Swamy, Decomposition of 2-propanol on an intermetallic compound for hydrogen storage, *React. Kinet. Catal. Lett.* 53 (1994) 429–440. doi:10.1007/BF02073052.
- [30] M.A. Aramendía, V. Boráu, I.M. García, C. Jiménez, A. Marinas, J.M. Marinas, A. Porras, F.J. Urbano, Comparison of different organic test reactions over acid–base catalysts, *Appl. Catal. Gen.* 184 (1999) 115–125. doi:10.1016/S0926-860X(99)00096-4.
- [31] K. Arata, H. Sawamura, The Dehydration and Dehydrogenation of Ethanol Catalyzed by TiO₂–ZrO₂, *Bull. Chem. Soc. Jpn.* 48 (1975) 3377–3378. doi:10.1246/bcsj.48.3377.
- [32] H. Pines, R.C. Olberg, V.N. Ipatieff, Studies in the Terpene Series. VIII.1 Effect of Catalyst, Solvent and Temperature on the Dehydrogenation of Pinane and p-Menthane, *J. Am. Chem. Soc.* 70 (1948) 533–537. doi:10.1021/ja01182a031.
- [33] Q.-H. Zhang, L. Gao, J.-K. Guo, Preparation and characterization of nanosized TiO₂ powders from aqueous TiCl₄ solution, *Nanostructured Mater.* 11 (1999) 1293–1300. doi:10.1016/S0965-9773(99)00421-3.
- [34] K.T. Jung, A.T. Bell, The effects of synthesis and pretreatment conditions on the bulk structure and surface properties of zirconia, *J. Mol. Catal. Chem.* 163 (2000) 27–42. doi:10.1016/S1381-1169(00)00397-6.
- [35] E.I. Ross-Medgaarden, W.V. Knowles, T. Kim, M.S. Wong, W. Zhou, C.J. Kiely, I.E. Wachs, New insights into the nature of the acidic catalytic active sites present in ZrO₂-supported tungsten oxide catalysts, *J. Catal.* 256 (2008) 108–125. doi:10.1016/j.jcat.2008.03.003.
- [36] K. Chen, S. Xie, E. Iglesia, A.T. Bell, Structure and Properties of Zirconia-Supported Molybdenum Oxide Catalysts for Oxidative Dehydrogenation of Propane, *J. Catal.* 189 (2000) 421–430. doi:10.1006/jcat.1999.2720.
- [37] A. Calafat, L. Avilán, J. Aldana, The influence of preparation conditions on the surface area and phase formation of MoO₃/ZrO₂ catalysts, *Appl. Catal. Gen.* 201 (2000) 215–223. doi:10.1016/S0926-860X(00)00441-5.
- [38] R. Srinivasan, T. Watkins, C. Hubbard, B.H. Davis, Sulfated Zirconia Catalysts. The Crystal Phases and Their Transformations, *Chem. Mater.* 7 (1995) 725–730. doi:10.1021/cm00052a018.
- [39] B.Y. Zhao, X.P. Xu, H.R. Ma, D.H. Sun, J.M. Gao, Monolayer dispersion of oxides and salts on surface of ZrO₂ and its application in preparation of ZrO₂-supported catalysts with high surface areas, *Catal. Lett.* 45 (1997) 237–244. doi:10.1023/A:1019048503124.
- [40] B.M. Reddy, P.M. Sreekanth, V.R. Reddy, Modified zirconia solid acid catalysts for organic synthesis and transformations, *J. Mol. Catal. Chem.* 225 (2005) 71–78. doi:10.1016/j.molcata.2004.09.003.
- [41] G. Tsilomelekis, A. Christodoulakis, S. Boghosian, Support effects on structure and activity of molybdenum oxide catalysts for the oxidative dehydrogenation of ethane, *Catal. Today.* 127 (2007) 139–147. doi:10.1016/j.cattod.2007.03.026.
- [42] T.I. Halkides, D.I. Kondarides, X.E. Verykios, Catalytic reduction of NO by C₃H₆ over Rh/TiO₂ catalysts, *Appl. Catal. B Environ.* 41 (2003) 415–426. doi:10.1016/S0926-3373(02)00176-5.

- [43] Z. Liu, Y. Chen, Spectroscopic studies on tetragonal ZrO₂-supported MoO₃ and NiO–MoO₃ systems, *J. Catal.* 177 (1998) 314–324. doi:10.1006/jcat.1998.2123.
- [44] G. Mestl, T.K.K. Srinivasan, Raman Spectroscopy of Monolayer-Type Catalysts: Supported Molybdenum Oxides, *Catal. Rev.* 40 (1998) 451–570. doi:10.1080/01614949808007114.
- [45] S. Xie, K. Chen, A.T. Bell, E. Iglesia, Structural Characterization of Molybdenum Oxide Supported on Zirconia, *J. Phys. Chem. B.* 104 (2000) 10059–10068. doi:10.1021/jp002419h.
- [46] P. Dufresne, E. Payen, J. Grimblot, J.P. Bonnelle, Study of nickel-molybdenum- γ -aluminum oxide catalysts by x-ray photoelectron and Raman spectroscopy. Comparison with cobalt-molybdenum- γ -aluminum oxide catalysts, *J. Phys. Chem.* 85 (1981) 2344–2351. doi:10.1021/j150616a010.
- [47] T. Ono, H. Miyata, Y. Kubokawa, Catalytic activity and structure of Mo oxide highly dispersed on ZrO₂ for oxidation reactions, *J. Chem. Soc. Faraday Trans. 1 Phys. Chem. Condens. Phases.* 83 (1987) 1761–1770. doi:10.1039/F19878301761.
- [48] H. Hu, I.E. Wachs, S.R. Bare, Surface Structures of Supported Molybdenum Oxide Catalysts: Characterization by Raman and Mo L₃-Edge XANES, *J. Phys. Chem.* 99 (1995) 10897–10910. doi:10.1021/j100027a034.
- [49] D.S. Kim, K. Segawa, T. Soeya, I.E. Wachs, Surface structures of supported molybdenum oxide catalysts under ambient conditions, *J. Catal.* 136 (1992) 539–553. doi:10.1016/0021-9517(92)90084-U.
- [50] B. Zhao, X. Wang, H. Ma, Y. Tang, Raman spectroscopy studies on the structure of MoO₃/ZrO₂ solid superacid, *J. Mol. Catal. Chem.* 108 (1996) 167–174. doi:10.1016/1381-1169(96)00008-8.
- [51] G. Tsilomelekis, S. Boghosian, On the configuration, molecular structure and vibrational properties of MoO_x sites on alumina, zirconia, titania and silica, *Catal. Sci. Technol.* 3 (2013) 1869–1888. doi:10.1039/C3CY00057E.
- [52] A. Gervasini, A. Auroux, Acidity and basicity of metal oxide surfaces II. Determination by catalytic decomposition of isopropanol, *J. Catal.* 131 (1991) 190–198. doi:10.1016/0021-9517(91)90335-2.
- [53] A.L. McKenzie, C.T. Fishel, R.J. Davis, Investigation of the surface structure and basic properties of calcined hydrotalcites, *J. Catal.* 138 (1992) 547–561. doi:10.1016/0021-9517(92)90306-3.
- [54] D. Dautzenberg, H. Knözinger, Influence of steric and inductive effects on product distributions in the dehydration of secondary alcohols on alumina, *J. Catal.* 33 (1974) 142–144. doi:10.1016/0021-9517(74)90254-1.
- [55] S.B. Chaabene, L. Bergaoui, A. Ghorbel, J.F. Lambert, P. Grange, Acidic properties of a clay prepared from the reaction of zirconyl chloride solution containing sulfate ions with montmorillonite, *Appl. Catal. Gen.* 252 (2003) 411–419. doi:10.1016/S0926-860X(03)00491-5.
- [56] P. Berteau, M. Ruwet, B. Delmon, Reaction Pathways in 1-Butanol Dehydration on γ -Alumina, *Bull. Sociétés Chim. Belg.* 94 (1985) 859–868. doi:10.1002/bscb.19850941113.
- [57] C. Martín, G. Solana, P. Malet, V. Rives, Nb₂O₅-supported WO₃: a comparative study with WO₃/Al₂O₃, *Catal. Today.* 78 (2003) 365–376. doi:10.1016/S0920-5861(02)00301-2.
- [58] C. Morterra, G. Ghiotti, E. Garrone, E. Fiescaro, Spectroscopic study of anatase properties. Part 3. Surface acidity, *J. Chem. Soc. Faraday Trans. 1 Phys. Chem. Condens. Phases.* 76 (1980) 2102–2113. doi:10.1039/F19807602102.
- [59] T.H. Ballinger, J.T. Yates, IR spectroscopic detection of Lewis acid sites on alumina using adsorbed carbon monoxide. Correlation with aluminum-hydroxyl group removal, *Langmuir.* 7 (1991) 3041–3045. doi:10.1021/la00060a022.
- [60] W. Turek, A. Krowiak, Evaluation of oxide catalysts' properties based on isopropyl alcohol conversion, *Appl. Catal. Gen.* 417–418 (2012) 102–110. doi:10.1016/j.apcata.2011.12.030.
- [61] K. Hadjiivanov, J.-C. Lavalley, FT–IR spectroscopic study of CO adsorption on monoclinic zirconia of different hydroxylation degrees, *Catal. Commun.* 2 (2001) 129–133. doi:10.1016/S1566-7367(01)00020-6.

- [62] C.D. Baertsch, K.T. Komala, Y.-H. Chua, E. Iglesia, Genesis of Brønsted Acid Sites during Dehydration of 2-Butanol on Tungsten Oxide Catalysts, *J. Catal.* 205 (2002) 44–57. doi:10.1006/jcat.2001.3426.
- [63] B. Samaranch, P. Ramírez de la Piscina, G. Clet, M. Houalla, N. Homs, Study of the Structure, Acidic, and Catalytic Properties of Binary Mixed-Oxide $\text{MoO}_3\text{-ZrO}_2$ Systems, *Chem. Mater.* 18 (2006) 1581–1586. doi:10.1021/cm052433c.

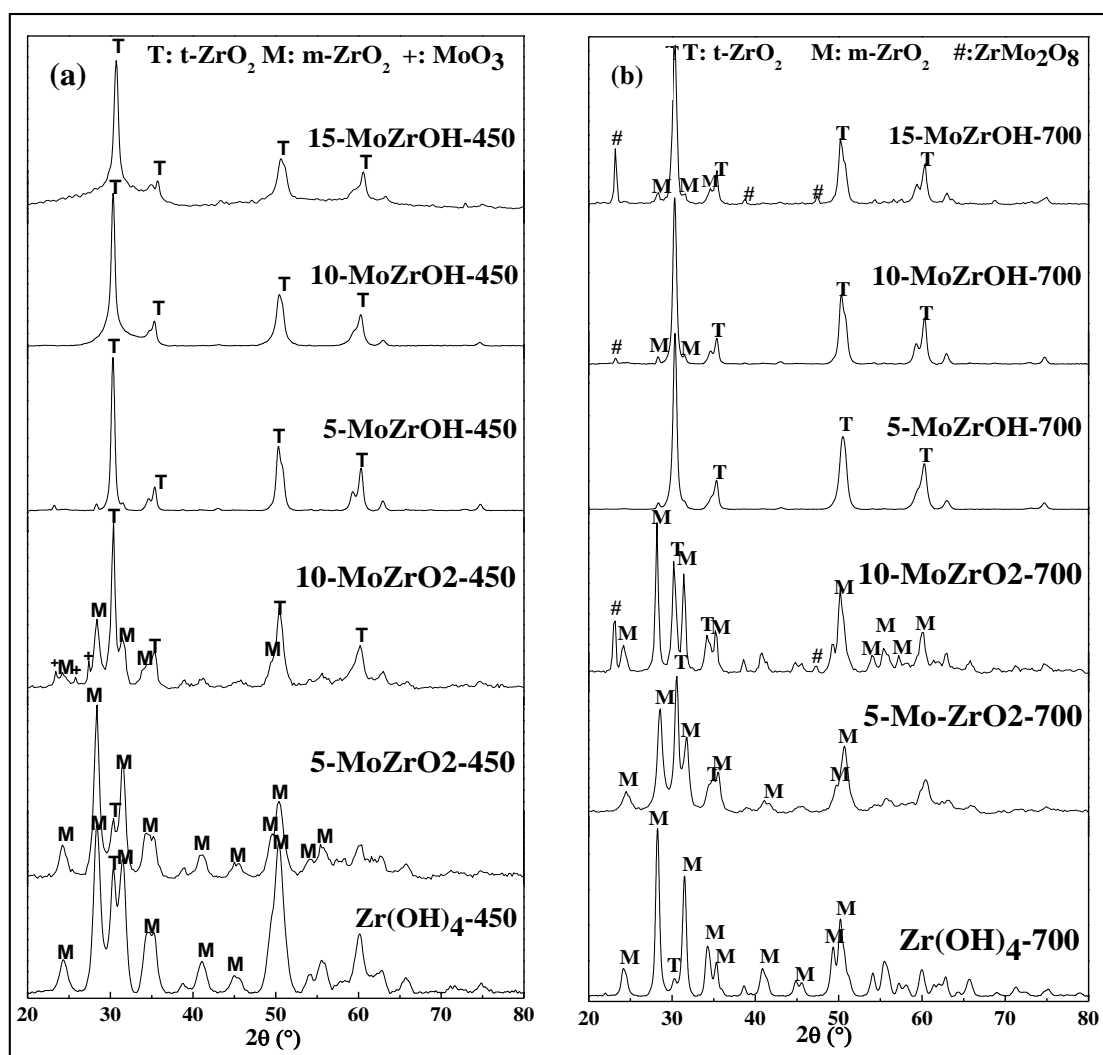


Figure 1. X-Ray diffraction patterns of pure ZrO₂ and Mo-Zr samples calcined at (a) 450°C and (b) 700°C.

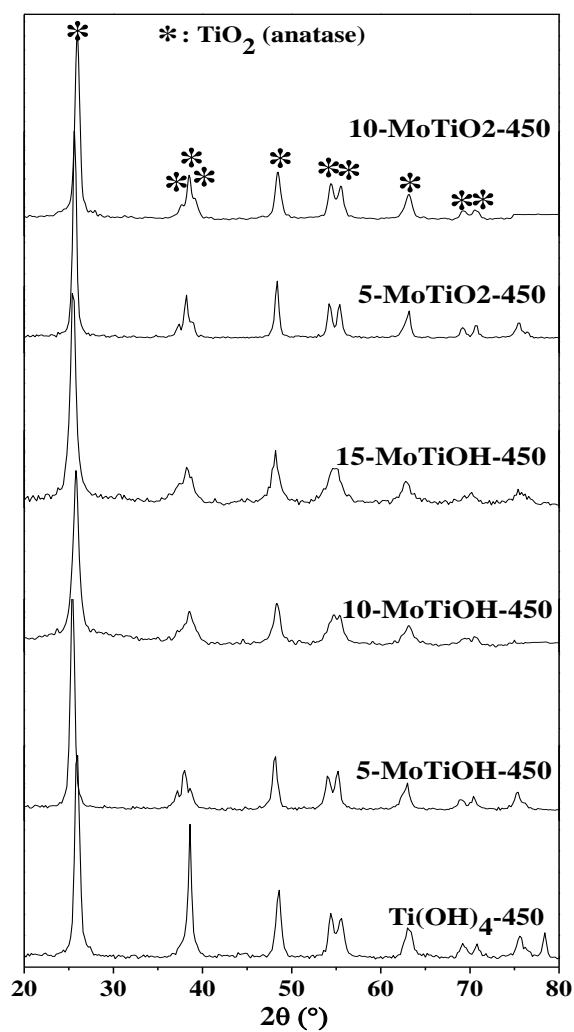


Figure 2. X-Ray diffraction patterns for pure TiO₂ and Mo-Ti solids calcined at 450°C.

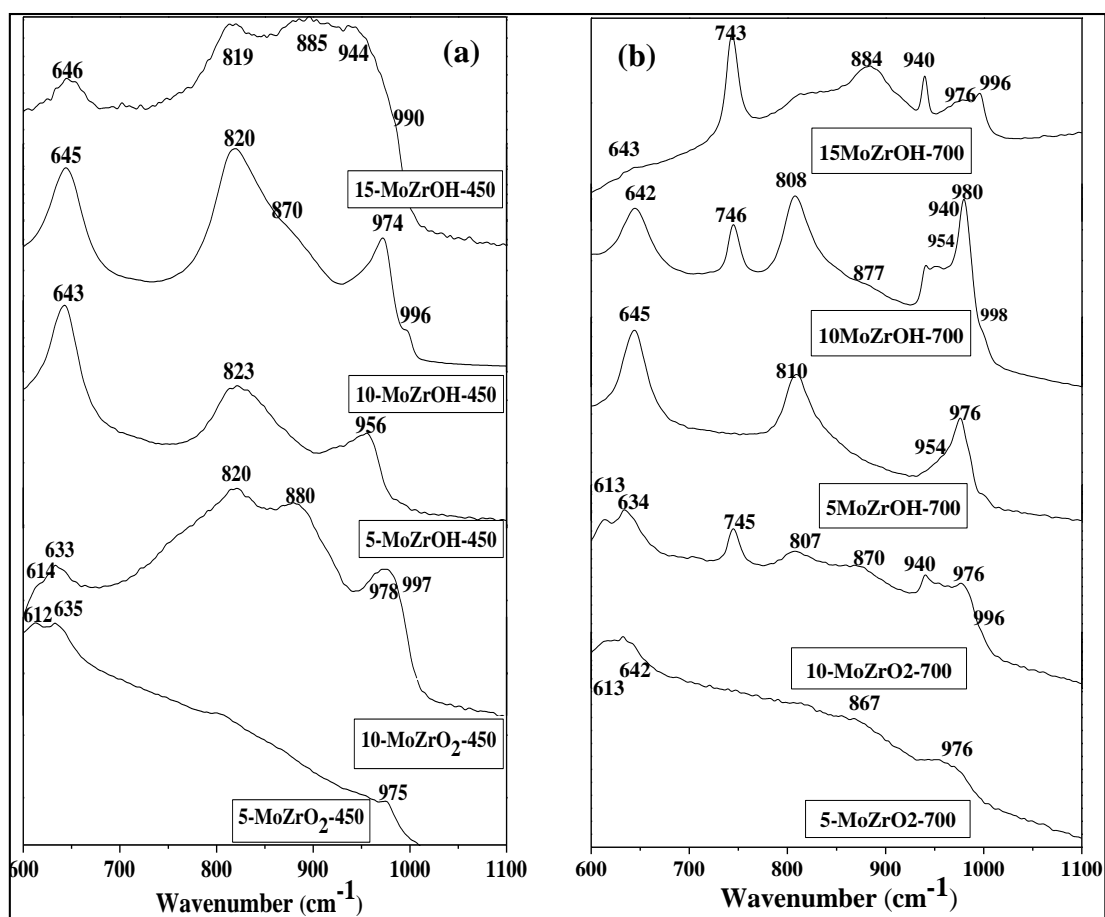


Figure 3. Raman spectra of zirconia supported molybdenum catalysts calcined at (a) 450°C and (b) 700°C.

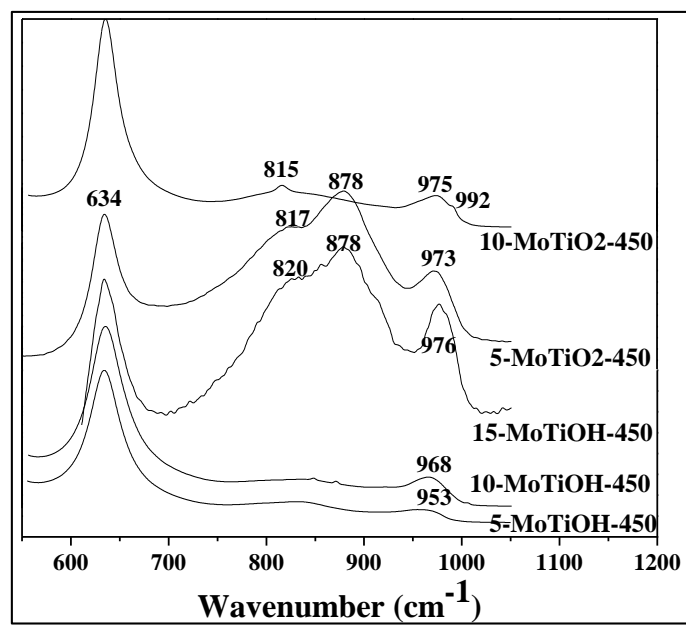


Figure 4. Raman spectra of Mo-Ti solids calcined at 450°C.

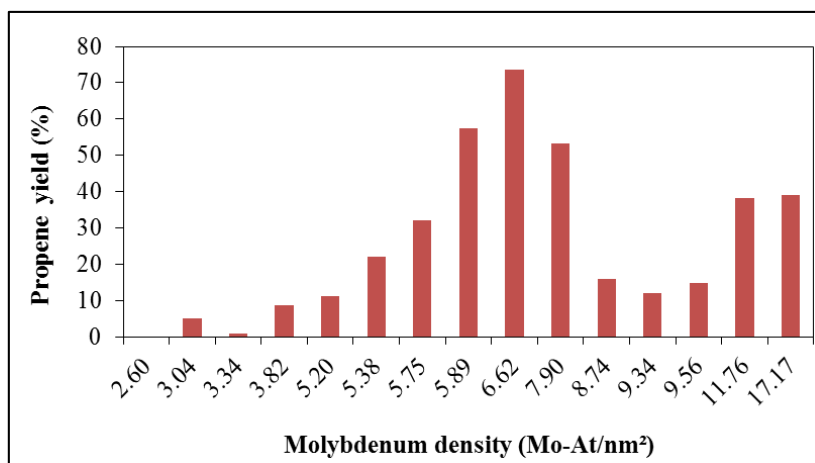


Figure 5. Propene yield as a function of surface molybdenum density.

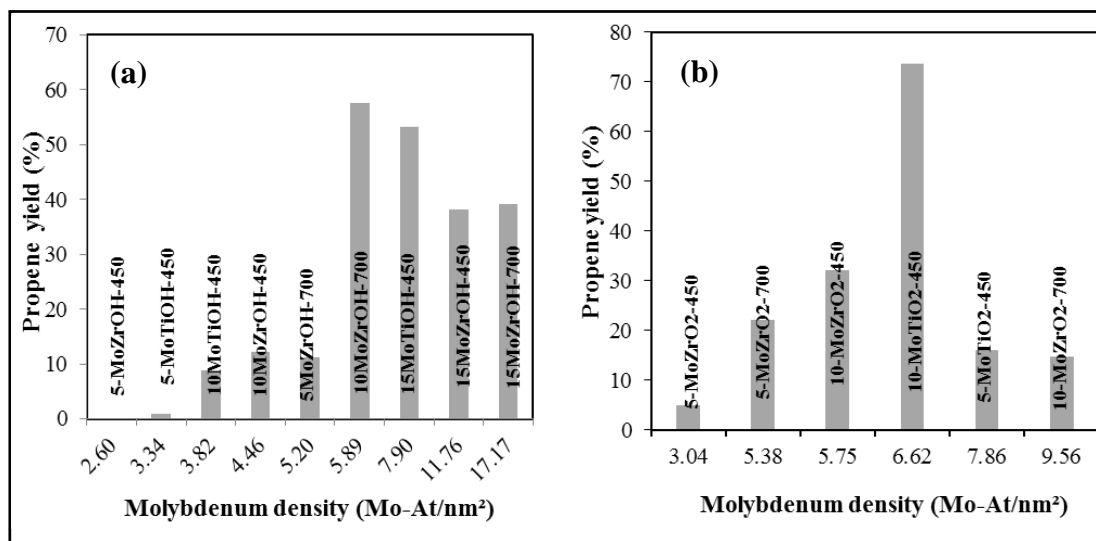


Figure 6. Propene yield as a function of molybdenum density; (a): hydroxide impregnation protocol; (b): oxide impregnation protocol.

Table 1. Physicochemical characteristics of zirconia, titania supports and of molybdenum supported solids.

Solids	Calcination temperature	%Mo ^a	t-ZrO ₂ (vol.%)	BET area (m ² /g)	surface Density ^b (Mo at/nm ²)
Mo-Zr catalysts					
ZrO₂-450	450	-	41	71	
5-MoZrOH-450	450	4.1	97	99	2.6
10-MoZrOH-450	450	7.9	100	111	4.5
15-MoZrOH-450	450	12.5	100	67	11.8
5-MoZrO₂-450	450	3.9	30	80	3.0
10-MoZrO₂-450	450	8.3	73	90	5.8
ZrO₂-700	700	-	11	25	-
5-Mo-ZrOH-700	700	4.1	100	49	5.2
10-MoZrOH-700	700	9.2	96	98	5.9
15-MoZrOH-700	700	10.2	94	37	17.2
5-MoZrO₂-700	700	4.1	60	47	5.4
10-MoZrO₂-700	700	8.1	47	53	9.6
Mo-Ti catalysts					
TiO₂-450	450	-		64	-
5-MoTiOH-450	450	5.0		93	3.3
10-MoTiOH-450	450	7		115	3.8
15-MoTiOH-450	450	11.8		93	7.9
5-MoTiO₂-450	450	5.1		37	8.7
10-MoTiO₂-450	450	7.7		73	6.6

^a: Determined from X-Ray Fluorescence analysis

^b: Calculated from the XRF molybdenum content value.

Table 2. Conversion and selectivities in the isopropanol decomposition reaction .

Solid	Surface Density (Mo-at/nm ²)	Conversion (%)	Propene selectivity (%)	Ether selectivity (%)	Acetone selectivity (%)
ZrO ₂ -450	-	Inactive	-	-	-
ZrO ₂ -700	-	Inactive	-	-	-
5-MoZrOH-450	2.6	Inactive	-	-	-
5-MoZrOH-700	5.2	17.1	65.8	32.9	1.3
10-MoZrOH-450	4.5	19.2	63.1	20.8	11
10-MoZrOH-700	5.9	59.6	96.6	2.8	0.6
15-MoZrOH-450	11.8	40.7	93.8	3.7	2.5
15-MoZrOH-700	17.2	39.1	100	0	0
5-MoZrO ₂ -450	3.04	9.5	53.1	15.5	31.4
5-MoZrO ₂ -700	5.4	26.6	83	10.8	6.2
10-MoZrO ₂ -450	5.8	37.8	85.2	10.1	4.7
10-MoZrO ₂ -700	9.6	17.3	85.2	10.7	4.1
TiO ₂ -450	-	Inactive	-	-	-
5-MoTiOH-450	3.3	1.4	58.2	27.9	10.4
10-MoTiOH-450	3.8	11.8	74.9	20.2	2.7
15-MoTiOH-450	7.9	56.1	95	2.2	2.8
5-MoTiO ₂ -450	8.7	21.3	75.1	16	9
10-MoTiO ₂ -450	6.6	74.8	98.4	0.9	0.7

Table 3: Propene and diisopropylether yields for solids with close molybdenum densities and prepared via different protocols

Iso-density (Mo-At/nm²)	~6		~8		~10	
Density value (Mo-At/nm²)	5.75	5.89	7.86	7.9	9.56	11.76
Solid	10MoZrO₂- 450	10MoZrOH- 700	5MoTiO₂- 450	15MoTiOH- 450	10MoZrO₂- 700	15MoZrOH- 450
Propene yield (%)	32.2	57.6	16	53.3	14.7	38.2
Diisopropylether yield (%)	3.8	1.7	3.4	1.2	1.9	1.5